

Design, Characterization, and Mechanical Programming of Fabric-Reinforced Textile Actuators for a Soft Robotic Hand

Pham H. Nguyen⁺, *Student Member, IEEE*, Francisco Lopez-Arellano⁺,
Wenlong Zhang^{*}, *Member, IEEE*, and Panagiotis Polygerinos, *Member, IEEE*

Abstract—In this paper, we present the design, fabrication, and evaluation of robust, fabric-reinforced textile actuators, which are capable of performing a variety and combination of motions, such as axial extension, radial expansion, bending, and twisting along its central axis. A simple fabrication procedure using a combination of lamination and sewing is described. The relationship between the fabric reinforcement characteristics and the actuator deformation is studied and experimentally verified. Multi-segment actuators can be created by tailoring different sections of fabric-reinforcements together in order to generate combination of motions to perform specific tasks. We demonstrate this by designing an anthropomorphic soft robotic hand and providing preliminary evaluations on grasping daily living objects of various size and shapes.

I. INTRODUCTION

Soft pneumatic actuators (SPAs) have been a cornerstone of soft robotics in a variety of applications such as mobile and assistive devices [1]. SPAs are generally lightweight, have a high power-to-weight ratio, are inexpensive to fabricate, compliant, and can safely interact with the user as well as the surrounding environment. SPAs are often classified based on the materials as well as the type of motion they can create [2]. These motions include bending, twisting, extending, contracting, and a combination of these [2]–[7]. Past work has established the design, fabrication, and mechanical programming of SPAs, in particular the soft elastomeric actuators, to generate a variety of movement using different forms of restraints, like Kevlar threads, origami shells, plastic shells, or rings [3], [4], [8]–[10].

A recent trend in SPAs, has been the introduction of textile or fabric-based actuators and robots [11]–[15]. Textiles have shown a lot of potential to create SPAs as they are naturally lightweight, conformable, collapsible, high-strength, stretchable, and intrinsically anisotropic [11], [13]. Recent research have seen non-stretchable, high-strength fabrics used to create bending actuators that are robust with a high power-to-weight ratio [14]–[16], as well as the use of stretchable textiles to create bending actuators for grippers and wearable robots [11], [13], [17].

This work was supported in part by the National Science Foundation under grant CMMI-1800940.

P. H. Nguyen, W. Zhang, and P. Polygerinos are with the Polytechnic School, Ira A. Fulton Schools of Engineering, Arizona State University, Mesa, AZ 85212, USA. nhpham2@asu.edu; wenlong.zhang@asu.edu; polygerinos@asu.edu

F. L. Arellano is with The School of Biological Health Systems Engineering, Ira A. Fulton Schools of Engineering, Arizona State University, Tempe, AZ 85281, USA. flopezar@asu.edu

⁺ P. H. Nguyen and F. L. Arellano are equally contributing authors.

^{*} Address all correspondence to this author.

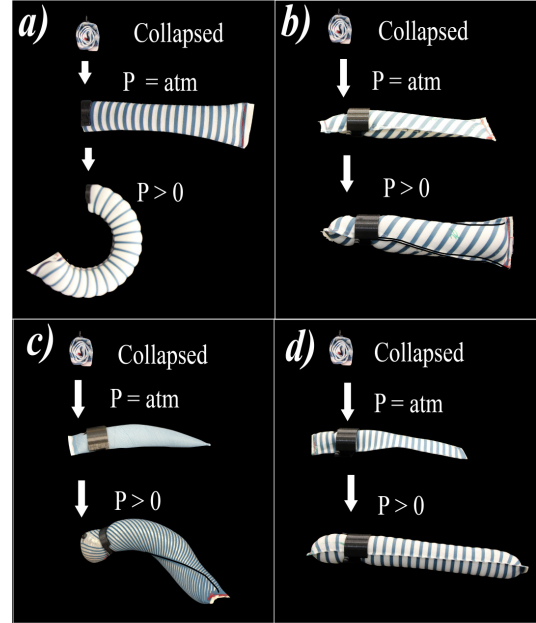


Fig. 1: FRTA going from collapsed/squeezed state, to deflated state ($P = atm$), to inflated state ($P > 0$). (a) Bending actuator, b) Twisting actuator, c) Bending-twisting actuator, and d) Extending actuator

In this paper, we introduce a new class of textile-based soft pneumatic actuators, called the fabric-reinforced textile actuators (FRTAs) that can be mechanically programmed using fabric reinforcements to perform bending, twisting along its central axis, extending, and a combination of these movements as shown in Fig. 1. By exploiting the material and geometrical properties of the stretchable knitted textile as well as the properties of the fabric reinforcements we can exhibit complex deformations. The fabrication method of these FRTAs eliminates the need of wrapping Kevlar threads or adding rings around the actuators, as seen in our previous work [4], [10]. Instead, the laser-cut fabric reinforcements are added along the body of the actuator using a single step lamination and layering process. The FRTAs are experimentally studied to provide design guidelines and help the soft robotics community understand how these soft actuators vary their outputs as a function of input pressure, material anisotropy, and geometrical parameters of the fabric reinforcements. Finally, we show that our manufacturing facilitates the design of actuators tailored to specific functions, as demonstrated by an anthropomorphic soft robotic hand with fingers made of multiple segments of FRTAs that can perform a combination of multiple movements in tandem.

The remainder of the paper is organized as follows.

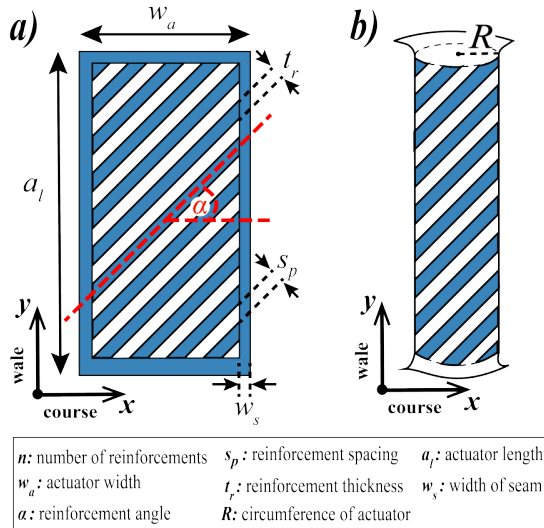


Fig. 2: Geometrical parameters of FRTAs

Section II introduces the design, material characterization, mechanical programming, and fabrication process of the FRTA. Section III evaluates FRTAs for varying geometrical parameters. Section IV presents the design, integration, and preliminary evaluation of the anthropomorphic soft hand. Section V concludes and discusses some future directions.

II. ACTUATOR DESIGN AND FABRICATION

In contrast to the elastomeric fiber-reinforced actuators [3], [4], [6], [18], FRTAs fabricated using knitted textiles have different stretch and strain properties in bi-directions, due to their intrinsic anisotropy. FRTAs are also lightweight and allow full collapsibility when not activated, to 13% of its original length, as seen in Fig. 1. The fabric reinforcements also reduce local stresses and strains, minimizing surface damage due to abrasion or cutting, seen with Kevlar threads. The fabrication method to construct these FRTAs require the use of 2D manufacturing methods, like sewing or laminating, to create 3D structures. In this section, we look at the fabric reinforcements to mechanically program the textile-based actuators to perform motions such as radial expansion, axial extension, twisting about its axis, extending-twisting, bending, and bending-twisting, upon pressurization.

A. Actuator Geometrical Parameters

To study the effects of the fabric reinforcements on the performance of the actuators as well as its ability to create complex motions, a set of geometrical parameters shown in Fig. 2 are analyzed. The high-stretch knitted textiles used, have stretchability in two different directions that are referred to as wale (in the y -direction) and course (in the x -direction) [11] seen in Fig. 2. In this paper, the two main geometrical parameters studied are the angle of the fabric reinforcements (α) and the number of fabric reinforcements (n). By α , the actuators are able to perform one or a combination of motions whether it is axial extension, radial expansion, or twisting about its axis. The relationship between the radius of the actuator (R) and the width of the actuator (w_a), is as seen in Eq. (1) below. The number of

fabrics reinforcements (n), is related to the thickness of the reinforcements (t_r), which is modifiable in the case of fabric reinforcements, in comparison to the fiber reinforcements, and the length of the actuator (a_l) as seen in Eq. (2) below:

$$R = \frac{(w_a - 2w_s)}{2\pi} \quad (1)$$

$$n = \frac{a_l \cdot \cos(\alpha)}{t_r + s_p}. \quad (2)$$

B. Material Properties and Mechanical Programmability

1) *Mechanical Properties*: We mechanically characterize the properties of the high-stretch textiles using a universal testing machine (UTM Instron 5944, Instron Corp., High Wycombe, United Kingdom) on both the uncoated knitted textile material and TPU coated/laminated knitted textile material. The uncoated and coated knitted textile materials are compared because the laminated layer of TPU coating increases the overall stiffness in both directions of the knitted textile. In this paper, the high stretch knitted textile (24350, Darlington Fabrics, Westerly, RI) is composed of 83% 50 Denier Semi-Dull Nylon and 17% 210 Denier Spandex fibers. Using the ISO-139134-1 standard, these knitted materials were tested in both the wale and course directions, as seen in Fig. 3. We notice that in the wale direction, parallel to the direction of manufacturing, the knit has a higher stretch of 426.8% at 72.41MPa. In the course direction, perpendicular to the direction of manufacturing, the stretch was stiffer at 240.1% at 73.14MPa. The TPU-laminated textile material showed an increase of an overall stiffness in both directions but still preserves of the mechanical anisotropic properties of the knitted textile material at 422.9% at 83.78MPa (in the wale direction) and 240.1% at 71.01MPa (in the course direction). The properties of the inextensible 200-Denier, TPU-coated nylon fabric used for the fabric-reinforcements were determined with the ASTM D882 standard as Young's modulus of $E = 498MPa$.

2) *Mechanical Programmability*: In this work, the focus is on actuators that use only a single family of reinforcements, in contrast to our previous work [4], [19] that also had an additional second family of reinforcements, arranged in a crisscross manner with the first set, to subdue any

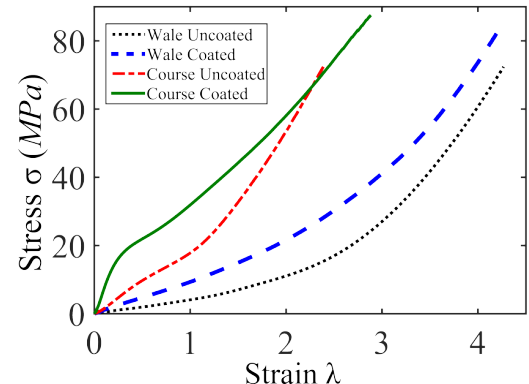


Fig. 3: Experimental stress-strain curves of the high-stretch textile Darlington Fabrics 24350

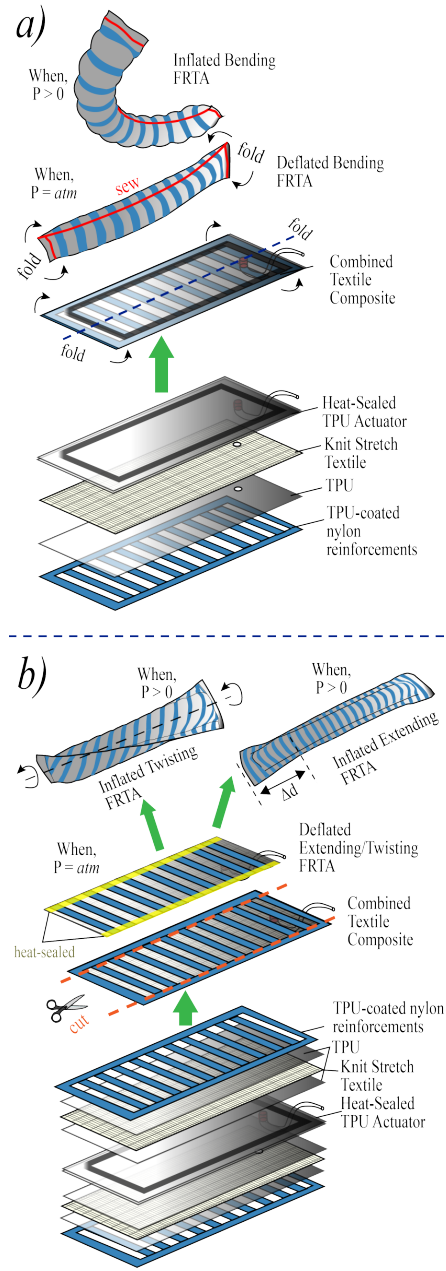


Fig. 4: (a) Fabrication of bending type FRTAs (b) Fabrication of extending and twisting type FRTAs

residual twisting motion (often because of manufacturing inaccuracies), in order to create pure extension or expansion, as shown in Fig. 1d). Pure extension (when $\alpha = 0^\circ$) and expansion can be achieved with the FRTAs using just a single family of reinforcements because the reinforcements are accurately laser-cut into shape and are easily aligned to laminate over the knitted textile shell, therefore reducing variability during fabrication. Additionally, the thicknesses of the fabric reinforcements (t_r) are modifiable to further reduce unwanted twisting motion. On the other hand, to create a pure twisting FRTA, seen in Fig. 1b), the angle of reinforcements (α) has to be larger (clockwise twist) or smaller (counterclockwise twist) than 0° .

In previous work [11], [13], [17], in order to create

a textile bending actuator, two different layers of fabrics are combined. The top layer is a high-stretch material and the bottom layer is inextensible. In our work, a bending FRTA, as seen in Fig. 1a), is created by sewing a superimposed seam (Seam Class-1) after folding the high-stretch textile laminated with fabric reinforcements, to act as the inextensible layer, as seen in Fig. 4. To create a pure bending FRTA, as shown in Fig. 1a), the reinforcement angle is set as $\alpha = 0^\circ$. A bending-twisting FRTA, as shown in Figure 1c), is created by setting $\alpha > 0^\circ$ for a clockwise and $\alpha < 0^\circ$ for a counterclockwise bend-twist motion instead.

C. Actuator Fabrication and Integration

To fabricate the FRTAs, the high-stretch knitted textile, TPU material (Fastelfilm 20093, Fastel Adhesive, Clemente, CA), and the TPU-coated nylon fabric (6607, Rockywoods Fabric, Loveland, CO), used as the fabric reinforcements, are cut into the desired shape using a laser-cutter (Glowforge Prof, Glowforge, Seattle, WA). There are two variations of the fabrication method, one for actuators that perform bending and bending-twisting and the other for actuators that extend, twist, and extend-twist, as shown in Fig. 4.

To create the bending actuators, as shown in Fig. 4a), the prepared TPU sheet is laminated over one side of the knitted textile to create an adhesive side, using a heat press (FLHP 3802, FancierStudio, Hayward, CA). This side is used to bond with the sheet of TPU-coated nylon fabric reinforcements using the heat press. A TPU actuator, heat-sealed using a custom CNC router, with a modified soldering iron tip (at 320°F), was introduced in our previous work [14]. Pneumatic fittings (5463K361, McMaster-Carr, Elmhurst, IL) are added. The combined textile composite, with the TPU actuator in between, is folded along the center and sewn to create a strain-limiting, inextensible centerline to allow bending. During inflation, the actuator bends towards the inextensible side to create the bending motion.

To create the extending and twisting actuators, as shown in Fig. 4b), layers of TPU sheets are laminated over both sides of knitted textile sheets. The external side of the sheets are bonded with sets of TPU-coated nylon fabric reinforcements. Although, the knitted textile is laminated with a double layer of TPU, some air leakage is noticed through the skin of the actuator during inflation. Therefore an additional TPU actuator is added in between the prepared knitted textile sheets with fabric reinforcements, to ensure air-impermeability. The edges of the combined textile composite, are heat-sealed using an impulse sealer (751143, Metronic, Seattle, WA). The heat-sealed edges still allow stretchability, so the actuators can extend or twist, reducing the need to sew a seam.

III. TESTING AND EVALUATION OF ACTUATORS

In this section, we test the FRTAs for the interaction between high-stretch knitted fabric and the fabric reinforcements to produce the bending, twisting, and extending motions with the varying internal pressure in the actuators. Each experiment was repeated three times. The actuators are

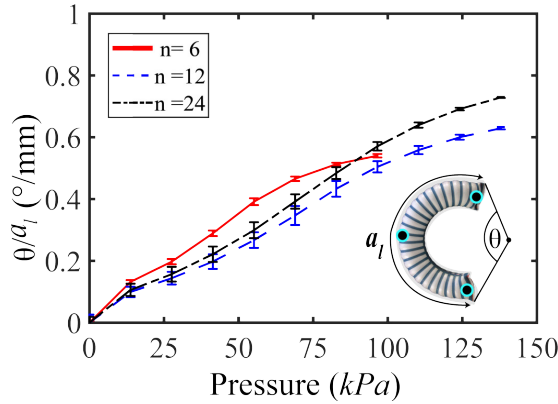


Fig. 5: Curvature angle per unit length for various numbers of fabric reinforcements (n). θ is the curvature angle and a_l is the curvature length of the actuator. Markers are signified by the blue dots.

designed with a set length ($a_l = 170\text{mm}$ and a set width $w_a = 30\text{mm}$). The bending and extending actuators are tested by varying the number of reinforcements (n) and the twisting actuators are tested by varying angle of reinforcements (α) using our motion capture system (Optitrack Prime 13W, NaturalPoint Inc., Corvallis, OR).

A. Bending Actuator

To study the performance bending, while varying the number of reinforcements ($n = 6, 12, 24$), three motion capture markers were added at the tip, mid-point, and base of each actuator to calculate the curvature angle (θ) of the actuator. The curvature length (a_l) is also monitored, and the curvature angle per unit length (θ/a_l) was calculated at each pressure interval, as seen in Fig. 5. The actuators were inflated up to 137.9kPa at increments of 13.8kPa . The bending curvatures (θ/a_l) at the maximum tested pressure, was $0.63^\circ/\text{mm}$, and $0.73^\circ/\text{mm}$ for $n = 12$ and 24 , respectively. The actuator with $n = 6$ showed uncontrolled radial expansion after the input pressure of 100kPa , leading to failure. It is also noticed that the bending curvature trend is very similar for these numbers of reinforcements. The difference between the performance of the bending actuators with the different reinforcement numbers were monitored with radial expansion, as seen in Fig. 6. The radial expansion was monitored using the final radius (R_f) over the initial radius (R_i). The actuators with the least number of reinforcements ($n = 6$) showed an radial expansion of up to 70% at 100kPa and the actuators with the

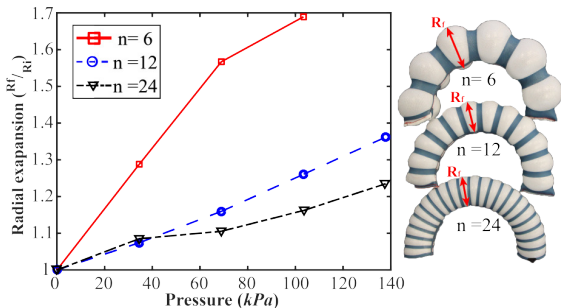


Fig. 6: Radial expansion for varying number of reinforcements. R_f is the final inflated radius and R_i is the initial radius.

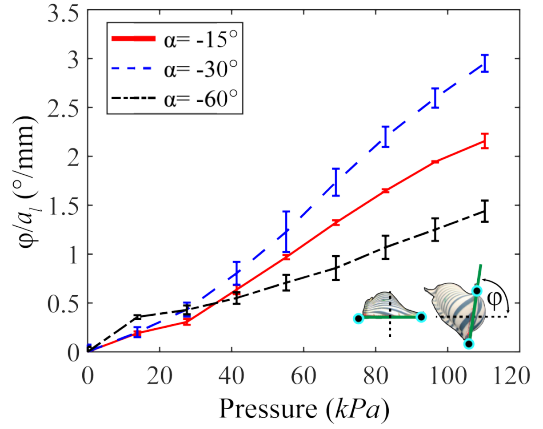


Fig. 7: Evaluation of the twisting capabilities of the FRTA for varying angle (ϕ). Markers are signified by the blue dots.

largest number of reinforcements showed just an increase of 24% at a higher pressure of 137.9kPa . Therefore, the more the reinforcements the larger the pressures the actuators can withstand, as well as the less the radial expansion, even though the bending performance is fairly similar.

B. Twisting Actuator

To study the effects of the fabric reinforcement angle ($\alpha = -15^\circ, -30^\circ, -60^\circ$) with the number of reinforcements ($n = 15$) on the twisting capability of the FRTAs, two markers were added along the width of the actuators at the tip and base of the actuators and the twisting angle (ϕ) per unit length (a_l) was monitored. The negative α means that the actuator is twisting in a counterclockwise manner. In this test, the FRTAs were inflated up to 110.316kPa in intervals of 13.789kPa , as shown in Fig. 7. The actuators with $\alpha = -15^\circ, -30^\circ, -60^\circ$, were able to twist up to $2.157^\circ/\text{mm}$, $1.44^\circ/\text{mm}$, and $2.951^\circ/\text{mm}$, respectively. This correlated to the actuators ($\alpha = -15^\circ, -30^\circ, -60^\circ$) twisting along its center axis up to 64.7° , 43.2° , and 87° at 110.316kPa . The least radial expansion observed for the twisting actuators, for $\alpha = -15^\circ$, was expanding 27.6% of its initial radius while the most prominent change in radius was achieved by $\alpha = -60^\circ$ reaching a radial expansion of 45.6 %. As it

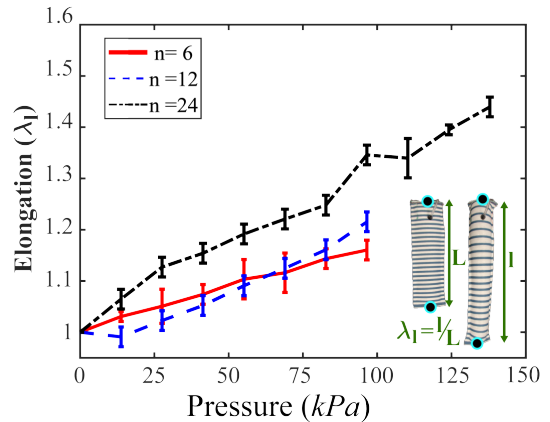


Fig. 8: Evaluation of the extension capabilities (λ_l) for varying number of reinforcements (n). Blue dots represent markers.

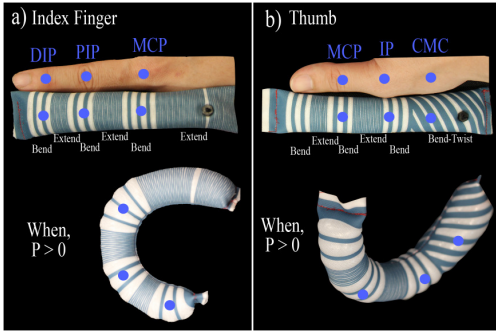


Fig. 9: a) Multi-segment FRTA to mimic the motion of the index finger. b) Multi-segment FRTA to mimic motion of the thumb.

can be observed not only the twist is affected by direction of the reinforcements but also the radial strain of the fiber. Therefore, the increase in α does not necessarily mean that the actuator will be able to twist better. We hypothesize, based on our previous work with fiber reinforcements [4], that the twisting performance of the actuator, clockwise or counterclockwise ($|\alpha|$), improves gradually from 0 to 30° and then the performance gradually reduces until $|\alpha| = 90^\circ$, where the reinforcements are symmetric and will not twist anymore, similarly to when $|\alpha| = 0^\circ$. At $110.316kPa$, the radial expansion increase was 27.6%, 30.1%, and 45.6% for $\alpha = -15^\circ, -30^\circ$, and -60° , respectively. Thus, the increase in twisting angle increases the radial expansion on the actuator as well.

C. Extending Actuator

To test the effects of the change in the number of reinforcement ($n = 6, 12, 24$) on the effects of bending, the extending actuators were tested up to $137.9kPa$ at increments of $13.8kPa$. Markers were placed on the tip and base of the actuators and the extension or elongation (λ_l) was monitored, as shown in Fig. 8. The actuators with $n = 6$ and 12, failed after $100kPa$. At $100kPa$, these actuators were able to stretch up to $\lambda_l = 1.16$ and 1.22. For the actuator with the most reinforcements $n = 24$, the maximum extension achieved was $\lambda_l = 1.44$ times more than its initial length. The trend for radial expansion followed a similar trend to the bending actuators, decreasing as the number of reinforcements increases. The results indicate that the actuators with $n = 6$ and 12 perform similarly. Furthermore, because



Fig. 10: Left: Deflated robotic hand. Right: Inflated robotic hand.

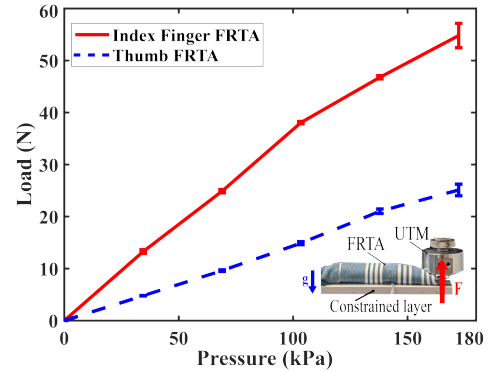


Fig. 11: Payload capability of the index finger and thumb inspired FRTA fingers, up till $172kPa$.

the radial expansion was prominent in these actuators, axial extension was affected and early failure was noticed. The radial expansion increase at $100kPa$, for $n = 6$ and 12 was 87.4% and 30.5%. To further convert radial expansion to axial extension, the number of reinforcements should be higher, as with the actuators with $n = 24$, where the radial expansion was 27.1% larger at a higher pressure of $137.4kPa$.

IV. ANTHROPOMORPHIC SOFT ROBOTIC HAND

To apply the capabilities of the FRTAs for grasping applications, an anthropomorphic soft robotic hand is designed inspired by the motion capabilities of the index finger and thumb of a biological human hand.

A. Design and Actuator Integration

The design of the fingers of the soft anthropomorphic robotic hand is based on two types of multi-segment FRTAs, as seen in Fig. 9. Multi-segment FRTAs, are actuators that can generate a combination of multiple mechanically programmed motions in series. The first multi-segment FRTA was designed based on motion mimicry of the index finger, by using only bending and extending segments, as shown in Fig. 9a). The bending sections aligned with the finger joints are the metacarpophalangeal (MCP), proximal interphalangeal (PIP), and distal interphalangeal (DIP). The extending sections are added to stretch the finger over the object it is trying to grasp. The second multi-segment FRTA was designed to follow the motion of the thumb, by making the base segment capable of bending-twisting, as shown in Fig. 9b). The bending-twisting motion allows the motion seen at the carpometacarpal (CMC) joint of the thumb.

The anthropomorphic hand design is highlighted in Fig. 10. It is made of four multi-segment, index finger inspired FRTAs and one thumb-inspired, FRTAs. Each finger is capped with a fabric pocket made of stretch fabric layered with grip material (3M TB614, 3M Company, Maplewood, MN) to allow a larger coefficient of friction during grasping. The palm of the hand is designed using a stretchable fingerless glove, where the fingers are secured in each slot. Foam is added to the center of the palm to provide a soft and compliant structure to the soft robotic hand. Each finger weighs only 7g and the soft robotic hand weighs 89g.

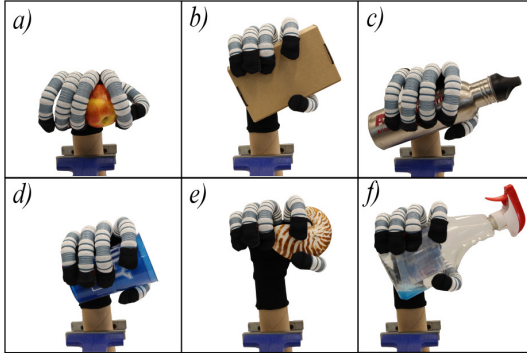


Fig. 12: a) Apple (168.5g) b) Box (134g) c) Metal Bottle (165g) d) Cup (50.3g) e) Sea Shell (94.1g) f) Cleaning Bottle (93g)

B. Preliminary Evaluation of Soft Robotic Hand

The payload capability of the fingers of the soft robotic hand was evaluated. The FRTAs were inflated upwards against the load cell of the UTM to measure the forces generated at the distal end of the multi-segment FRTAs, as shown in Fig. 11. The output is measured by varying the pressure up till 172kPa at intervals of 34.5kPa. The index finger and the thumb inspired FRTAs were capable of producing $54.8 \pm 2.36N$ and $25.1 \pm 1.13N$, respectively.

The grasping performance of the anthropomorphic soft robotic hand was preliminary evaluated by grasping six daily living objects of different weights, sizes, and textures. The objects tested include: an apple (168.5g), a box (134g), a metal bottle (165g), a cup (50.3g), a sea shell (94.1g), cleaning bottle (93g), shown in Fig 12. The fingers of the soft robotic hand was inflated up to a maximum of 172kPa.

V. CONCLUSION AND FUTURE WORK

In this paper, we presented the design, development, characterization, fabrication, and evaluation of new fabric-reinforced textile actuators (FRTAs) that could perform a combination of motions by exploiting the mechanical anisotropy of the knit textile material and its interaction with the fabric reinforcements. The geometrical parameters of the FRTAs were explored experimentally in order to provide guidelines to design these actuators for the desired motion when activated by input pressure. A manufacturing process was explored to allow accurate and rapid addition of fabric reinforcements using laser cutting and layered lamination. Finally, this paper reported the preliminary steps towards the development of a soft robotic anthropomorphic hand.

To further develop the soft robotic hand, additional payload testing of the grasp strength is required. The fingers will also be evaluated for grasping speed. In addition, more anthropomorphic grasp taxonomies will be explored (e.g. pinch grasping) with the use of the opposable thumb.

Future work will also include computational and analytical modeling of the dynamic responses of these actuators to allow evaluation of the actuators pre-fabrication. These models will be designed to optimize the geometrical parameters and material properties of the FRTAs based on the force output and desired motion in 3D space of multi-segment FRTAs as well as combinations of multiple FRTAs. This design tool can

also be further developed to design the mutli-segment FRTAs based on the task they perform as well. Future research will also seek to understand the nonlinear behavior of the textiles complex stretch deformation to create closed-loop motion control strategies.

REFERENCES

- [1] P. Polygerinos, N. Correll, S. A. Morin, B. Mosadegh, C. D. Onal, K. Petersen, M. Cianchetti, M. T. Tolley, and R. F. Shepherd. Soft Robotics: Review of Fluid-Driven Intrinsically Soft Devices; Manufacturing, Sensing, Control, and Applications in Human-Robot Interaction. *Advanced Engineering Materials*, 19(12):e201700016.
- [2] A. D. Marchese, R. K. Katzschmann, and D. Rus. A recipe for soft fluidic elastomer robots. *Soft Robotics*, 2(1):7–25, 2015. PMID: 27625913.
- [3] F. Connolly, C. J. Walsh, and K. Bertoldi. Automatic design of fiber-reinforced soft actuators for trajectory matching. *Proceedings of the National Academy of Sciences*, 114(1):51–56, 2017.
- [4] P. Polygerinos, Z. Wang, J. T. B. Overvelde, K. C. Galloway, R. J. Wood, K. Bertoldi, and C. J. Walsh. Modeling of Soft Fiber-Reinforced Bending Actuators. *IEEE Transactions on Robotics*, 31(3):778–789, 2015.
- [5] K. Suzumori, S. Iikura, and H. Tanaka. Development of flexible microactuator and its applications to robotic mechanisms. In *Proceedings. 1991 IEEE International Conference on Robotics and Automation*, number April, pages 1622–1627, apr 1991.
- [6] J. Bishop-Moser and S. Kota. Design and Modeling of Generalized Fiber-Reinforced Pneumatic Soft Actuators. *IEEE Transactions on Robotics*, 31(3):536–545, jun 2015.
- [7] D. Bruder, A. Sedal, R. Vasudevan, and C. D. Remy. Force generation by parallel combinations of fiber-reinforced fluid-driven actuators. *IEEE Robotics and Automation Letters*, 3(4):3999–4006, Oct 2018.
- [8] L. Paez, G. Agarwal, and J. Paik. Design and analysis of a soft pneumatic actuator with origami shell reinforcement. *Soft Robotics*, 3(3):109–119, 2016.
- [9] G. Agarwal, N. Besuchet, B. Audergon, and J. Paik. Stretchable Materials for Robust Soft Actuators towards Assistive Wearable Devices. *Scientific Reports*, 6(1):34224, 2016.
- [10] P. H. Nguyen, C. Sparks, S. G. Nuthi, N. M. Vale, and P. Polygerinos. Soft Poly-Limbs: Toward a New Paradigm of Mobile Manipulation for Daily Living Tasks. *Soft Robotics*, page soro.2018.0065, 2018.
- [11] F. Connolly, D. A. Wagner, C. J. Walsh, and K. Bertoldi. Sew-free anisotropic textile composites for rapid design and manufacturing of soft wearable robots. *Extreme Mechanics Letters*, 27:52 – 58, 2019.
- [12] Y. Fei, J. Wang, and W. Pang. A novel fabric-based versatile and stiffness-tunable soft gripper integrating soft pneumatic fingers and wrist. *Soft Robotics*, 2018.
- [13] L. Cappello, K. C. Galloway, S. Sanan, D. A. Wagner, R. Granberry, S. Engelhardt, F. L. Haufe, J. D. Peisner, and C. J. Walsh. Exploiting textile mechanical anisotropy for fabric-based pneumatic actuators. *Soft Robotics*, 5(5):662–674, 2018. PMID: 30024312.
- [14] P. H. Nguyen, I. B. Mohd Imran, C. Sparks, F. L. Arellano, W. Zhang, and P. Polygerinos. Fabric soft poly-limbs for physical assistance of daily living tasks. In *2019 IEEE International Conference on Robotics and Automation (ICRA)*, pages 8429–8435, May 2019.
- [15] H. K. Yap, P. M. Khin, T. H. Koh, Y. Sun, X. Liang, J. H. Lim, and C. Yeow. A fully fabric-based bidirectional soft robotic glove for assistance and rehabilitation of hand impaired patients. *IEEE Robotics and Automation Letters*, 2(3):1383–1390, July 2017.
- [16] P. H. Nguyen, S. Sridar, S. Amatya, C. Thalman, and P. Polygerinos. Fabric-based soft grippers capable of selective distributed bending for assistance of daily living tasks. In *2019 IEEE International Conference on Soft Robotics (RoboSoft)*, pages 404–409, April 2019.
- [17] G. Miron, B. Bdard, and J. S. Plante. Sleeved bending actuators for soft grippers: A durable solution for high force-to-weight applications. *Actuators*, 7(3), 2018.
- [18] G. Singh and G. Krishnan. An isoperimetric formulation to predict deformation behavior of pneumatic fiber reinforced elastomeric actuators. In *2015 IEEE/RSJ International Conference on Intelligent Robots and Systems (IROS)*, pages 1738–1743, Sep. 2015.
- [19] P. Polygerinos, Z. Wang, K. C. Galloway, R. J. Wood, and C. J. Walsh. Soft robotic glove for combined assistance and at-home rehabilitation. *Robotics and Autonomous Systems*, 73:135 – 143, 2015. Wearable Robotics.